Exploitation of missing linker in Zr-based metal-organic framework as the catalyst support for selective oxidation of benzyl alcohol

AUTHOR(S):

Jumpathong, Watthanachai; Pila, Taweesak; Lekjing, Yuwanda; Chirawatkul, Prae; Boekfa, Bundet; Horike, Satoshi; Kongpatpanich, Kanokwan

CITATION:

Jumpathong, Watthanachai ...[et al]. Exploitation of missing linker in Zr-based metal-organic framework as the catalyst support for selective oxidation of benzyl alcohol. APL Materials 2019, 7(11): 111109.

ISSUE DATE:

2019-11

URL:

http://hdl.handle.net/2433/244876

APL Materials

Exploitation of missing linker in Zr-based metal-organic framework as the catalyst support for selective oxidation of benzyl alcohol

Cite as: APL Mater. **7**, 111109 (2019); https://doi.org/10.1063/1.5126077
Submitted: 31 August 2019 . Accepted: 23 October 2019 . Published Online: 19 November 2019

Watthanachai Jumpathong, Taweesak Pila, Yuwanda Lekjing, Prae Chirawatkul, Bundet Boekfa, Satoshi Horike, and Kanokwan Kongpatpanich

APL Materials ARTICLE scitation.org/journal/apm

Exploitation of missing linker in Zr-based metal-organic framework as the catalyst support for selective oxidation of benzyl alcohol

Cite as: APL Mater. 7, 111109 (2019); doi: 10.1063/1.5126077
Submitted: 31 August 2019 • Accepted: 23 October 2019 •
Published Online: 19 November 2019

Watthanachai Jumpathong,[1,2] Taweesak Pila,[1,3,4] Yuwanda Lekjing,[1] Prae Chirawatkul,[5] Bundet Boekfa,[6] Satoshi Horike,[1,7,8,9,a)] and Kanokwan Kongpatpanich[1,4,a)]

AFFILIATIONS

[1]Department of Materials Science and Engineering, School of Molecular Science and Engineering, Vidyasirimedhi Institute of Science and Technology, Rayong 21210, Thailand
[2]Program on Chemical Biology, Chulabhorn Graduate Institute, Laksi, Bangkok 10210, Thailand
[3]Department of Chemical and Biomolecular Engineering, School of Energy Science and Engineering, Vidyasirimedhi Institute of Science and Technology, Rayong 21210, Thailand
[4]Research Network of NANOTEC-VISTEC on Nanotechnology for Energy, Vidyasirimedhi Institute of Science and Technology, Rayong 21210, Thailand
[5]Synchrotron Light Research Institute (Public Organization), Nakhon Ratchasima 30000, Thailand
[6]Department of Chemistry, Faculty of Liberal Arts and Science, Kasetsart University, Kamphaengsean Campus, Nakhonpathom 73140, Thailand
[7]Institute for Integrated Cell-Material Sciences (iCeMS), Institute for Advanced Study, Kyoto University, Kyoto 606-8501, Japan
[8]Department of Synthetic Chemistry and Biological Chemistry, Graduate School of Engineering, Kyoto University, Kyoto 615-8510, Japan
[9]AIST-Kyoto University Chemical Energy Materials Open Innovation Laboratory (ChEM-OIL), National Institute of Advanced Industrial Science and Technology (AIST), Yoshida-Honmachi, Sakyo-ku, Kyoto 606-8501, Japan

Note: This paper is part of the Special Topic on Open Framework Materials for Energy Applications.
[a)]**Authors to whom correspondence should be addressed:** horike@icems.kyoto-u.ac.jp and kanokwan.k@vistec.ac.th

ABSTRACT

Extensive studies have been done on the modification of the organic linkers with different functional groups for ameliorating the properties of Zr-based metal-organic frameworks (MOFs). In contrast, little effort has been devoted to Zr MOF modification at the –OH group arising from the incomplete coordination of Zr with the organic linkers. We focused on covalently immobilizing redox-active iron to the –OH group in the node of a Zr-based MOF for selective oxidation of benzyl alcohol to benzaldehyde, which is an important reaction in organic synthesis, pharmaceutical, and industrial areas. In this work, iron acetylacetonate was incorporated into $Zr_6(\mu_3\text{-}O)_4(\mu_3\text{-}OH)_4(HCOO)_6$(1,3,5-benzenetricarboxylate)$_2$ or MOF-808. The air-stable Fe-anchored MOF-808 (Fe-MOF-808) was subjected to screening for the selective oxidation of benzyl alcohol to benzaldehyde. Fe-MOF-808 showed enhanced conversion and selectivity to benzaldehyde as well as catalytically outperforming the pristine MOF-808 in the reaction. The prepared solid catalyst also displayed the robustness without the leaching of the active site during the reaction, along with at least four-time recyclability of use without significant deactivation.

INTRODUCTION

Selective oxidation of alcohol to aldehyde is of great importance in both academic research and industries. Benzaldehyde is one of the most industrially useful aromatic aldehydes that can be applied in the synthesis of many pharmaceutical drugs, agrochemicals, perfumes, and food additives.[1] The major concern in the production of benzaldehyde is the overoxidation of benzaldehyde to benzoic acid. Still, the commercial process for manufacturing benzaldehyde employs the chlorination of toluene to generate benzyl chloride, followed by hydrolysis and oxidation to yield benzaldehyde, which generates toxic halogenated wastes.[2] Noble metal clusters including Au, Pd, and Au–Pd bimetallic systems have been developed as catalysts for halogen-free production of benzaldehyde from biomass-derived benzyl alcohol.[3–6] The use of inexpensive redox-active metals such as Fe-based catalysts offers a good alternative although they are still scarcely reported in comparison to the precious metal catalysts. Fe-based compounds are redox-active species and are capable of catalyzing numerous selective oxidations in a similar fashion to Fe-containing metalloenzymes in biological processes.[7–9] In particular, Fe complexes have been reported for their potential use as homogeneous catalysts for the oxidation of benzyl alcohol to benzaldehyde.[10–14] The impregnation of Fe-based catalytic sites on a proper solid support to generate heterogeneous catalysts would yield promising catalytic activity and reusability.

Metal-organic frameworks (MOFs) or porous coordination polymers (PCPs) are a chimeric porous network composed of organic linkers and inorganic nodes.[15–17] MOFs have shown their versatile applications such as gas sorption, gas separation, drug delivery, chemical sensing, and heterogeneous catalysis.[18–21] Although a heterogeneous catalyst developed from Pd nanoclusters encapsulated in $Zr_6(\mu_3\text{-}O)_4(\mu_3\text{-}OH)_4$(1,4-benzenedicarboxylate)$_6$ (UiO-66) functionalized by $-NH_2$ groups was reported with yields of benzaldehyde up to 99%,[22] the metal used in the reaction was made from noble metals. An alternative catalytic site from natural abundant Fe^{3+} would be highly desirable. Recently, compelling evidence has been obtained to support that Zr-based MOFs have intrinsic defects at Zr nodes from the missing linker that are feasible for the incorporation of the desired functional groups.[23–27] The –OH group at the missing linker region offers the plausibility to covalently anchoring Fe catalytic sites to MOFs in an analogous fashion to those conventional metal-oxo supports such as silica, alumina, and zirconia.[28–30] A robust Zr-based MOF, $Zr_6(\mu_3\text{-}O)_4(\mu_3\text{-}OH)_4(HCOO)_6$(1,3,5-benzenetricarboxylate)$_2$ or MOF-808, is an intriguing choice of MOFs toward Fe impregnation at the Zr node owing to its sufficient large pore aperture (~16.6 Å) for substrate diffusion.[31]

In this work, the deposition of iron acetylacetonate precursors on the defective Zr node of MOF-808 was conducted to explore the cheap and readily available MOFs for selective oxidation of benzyl alcohol to benzaldehyde. The simplified grafting method provides an air-stable Fe-grafted MOF-808 that exhibited exceptional catalytic ability in terms of complete conversion and excellent selectivity. In addition, Fe-grafted MOF-808 was robust without leaching and can be reused at least four times.

MATERIALS AND METHODS

Materials

Zirconium oxychloride octahydrate ($ZrOCl_2{\cdot}8H_2O$), formic acid, and iron (III) chloride hexahydrate ($FeCl_3{\cdot}6H_2O$) were purchased from Merck. 1,3,5-benzenetricarboxylic acid (H_3BTC) and acetonitrile (HPLC grade) were purchased from Sigma-Aldrich. Other reagents and solvents were obtained commercially. Ultrapure deionized water (18.2 MΩ cm resistivity) used in HPLC was further filtered with PURELAB CLASSIC (Fisher Scientific).

Characterization

X-ray diffraction spectra were collected using Bruker D8 ADVANCE X-ray diffractometer using Cu $K\alpha$ radiation (40 kV, 40 mA, λ = 1.5418 Å). N_2 sorption isotherms at −196 °C were measured by Belsorp mini II with liquid nitrogen as a coolant. The pore size distribution of MOF-808 and Fe-MOF-808 were determined from N2 adsorption isotherms using the nonlocalized density functional theory (NLDFT) method and applying the cylindrical model. Infrared spectra were collected using Fourier transform infrared (FT-IR) spectrometer Frontier in the attenuated total reflectance (ATR) mode by scanning wavenumbers from 400 to 4000 cm^{-1}. Scanning electron microscopy (SEM) images and energy dispersive spectroscopy (EDS) line scans were collected using JEOL JSM-7610F. All samples were spluttered with platinum at 10 mA for 40 s prior to the imaging. Fe *K*-edge X-ray absorption near-edge structure (XANES) and Extended X-ray absorption fine structures (EXAFS) spectra were collected in the fluorescent mode at the beamline 1.1W of the Synchrotron Light Research Institute (SLRI), Thailand. The sample was calibrated with the Fe foil standard (7112 eV) to correct the energy value. The data processing and analysis were conducted by using the Athena and Artemis software package.[32] In the EXAFS fit, the S_0^2 is set to 1 for all correlations. Due to the lack of number of variables, σ^2 of all correlations were set to a single value, and only interatomic distances were varied independently. The EXAFS model was drawn using VESTA software,[33] and structural optimization was performed on Q-Chem software.[34] The $FeC_{57}Zr_6O_{36}H_{53}$ cluster was used to represent the Fe-MOF-808 catalysts. The cluster was optimized with the M06-L functional. The 6-31G(d,p) basis set was chosen to describe C, H, and O atoms, while the LANL2DZ basis set was applied for the Fe and Zr atoms. HPLC analysis was performed using Shimadzu Prominence-I (LC-2030 3D) with the C18 analytical column (1.5 × 150 mm, Dionex Acclaimed Polar Advantage II).

Syntheses of MOF-808 and Fe-MOF-808

MOF-808 was synthesized by the solvothermal method as described previously.[35] H_3BTC (0.315 g), $ZrOCl_2{\cdot}8H_2O$ (0.727 g), formic acid (33.7 ml), and *N*,*N*-dimethylformamide (DMF, 33.7 ml) were mixed in a Teflon autoclave. After that, the suspension was ultrasonicated for 2 min and subjected to constant heat in an oven at 130 °C for 48 h. The obtained white precipitate was washed with DMF, water, and acetone, respectively. The product was dried in a vacuum oven at 150 °C for 24 h to obtain the guest-free MOF-808. For Fe-MOF-808, 100 mg of guest-free MOF-808 and 4 M equivalence of $Fe(acac)_3$ were added with 40 ml DMF in a 100 ml glass

bottle. The suspension was sonicated for 5 min. Then, 100 μl of NEt_3 was added, and the resulting mixture was put in an oven at 80 °C for 48 h. The obtained MOF was centrifuged at 10 000 rpm for 5 min and the powder of MOF was collected. After that, the powder was further washed twice with DMF and twice with acetone. The resulting Fe-MOF-808 was dried in a vacuum oven at 80 °C and activated at 150 °C prior to further use.

Catalytic reaction, leaching, and recyclability tests

To a solution of benzyl alcohol (20.0 mg) in acetonitrile (10.0 ml) in a 50-ml round bottom flask, Fe-MOF-808 (10 mol. %) was added, and the suspension was ultrasonicated for 2 min. After that, 2 M equivalents of 70% aqueous tert-butylhydroperoxide (TBHP) were added, and the reaction mixture was allowed to stir for 9 h at 90 °C under the reflux condition. The reaction was quenched by adding MeOH and further analyzed using HPLC. For the leaching test, the solid catalyst (Fe-MOF-808) was separated from the host solution after reaction for 3 h. The filtrate was continued in the absence of the solid catalyst for additional 9 h. For the recyclability test, the catalyst was separated by centrifugation at the end of the reaction, and the pellet of the catalyst was collected. The solid catalyst was reused in the second run under the same reaction conditions. The catalyst did not show significant loss of the activity after four cycle runs. Power X-ray diffraction (PXRD) of the reused catalyst showed the intact structure after four catalytic cycles.

RESULTS AND DISCUSSION

MOF-808 possesses the –OH sites at the Zr node that can act as a molecular scaffold for covalent immobilization of desired active metals via atomic layer deposition in MOFs[23,24] and solvothermal deposition in MOFs[25,26] to generate the catalyst for various types of reactions. In this work, the grafting of the Fe complex was demonstrated by simply heating under air, and this resulted in an air-stable Fe-anchored MOF catalyst. MOF-808 was synthesized by the conventional solvothermal method and obtained as a white precipitate powder. One formate coordinated to the $Zr_6(\mu_3\text{-}O)_4(\mu_3\text{-}OH)_4$ node of MOF-808 was removed upon activation by heating under vacuum to create the –OH group (Fig. 1).

Iron acetylacetonate [$Fe(acac)_3$] was used as a precursor for the covalent attachment of the Fe^{3+} catalytic site at the –OH group of the Zr node. The grafting required triethylamine (NEt_3) as a strong base to facilitate the ligand exchange between acetylacetonate and the –OH node. Similar ligand exchange has been achieved in $Zr_6(\mu_3\text{-}O)_4(\mu_3\text{-}OH)_4$(1,4-benzenedicarboxylate)$_6$ or UiO-66 grafted by vanadium acetylacetonate.[26] After grating, the Brunauer–Emmett–Teller (BET) surface area of the obtained Fe-MOF-808 calculated from the N_2 adsorption isotherm decreases compared to that of pristine MOF-808 [Fig. 2(a)], suggesting the incorporation of the Fe complex inside the pore of MOF-808. Pore size distribution analysis from N_2 adsorption isotherms at 77 K also indicates smaller pore size as the internal pore space of MOF-808 is partially occupied by grafted Fe species. The crystal structure of MOF-808 is maintained after metal impregnation according to the power X-ray diffraction (PXRD) study [Fig. 2(b)].

To analyze the morphology of MOF-808 after reacting chemically with $Fe(acac)_3$, scanning electron microscopy (SEM) images were collected, and they show the intact morphologies of Fe-MOF-808 (Fig. 3). The energy dispersive spectroscopy (EDS) also reveals that the incorporation of iron species into the MOF framework is homogeneously distributed with 0.86 Fe incorporation per one Zr node. Elemental composition of the digested Fe-MOF-808 obtained from inductively coupled plasma optical emission spectrometry (ICP-OES) agrees with that quantified by EDS with the metal loading of 1.25 Fe/Zr node or approximately one Fe complex per one Zr node.

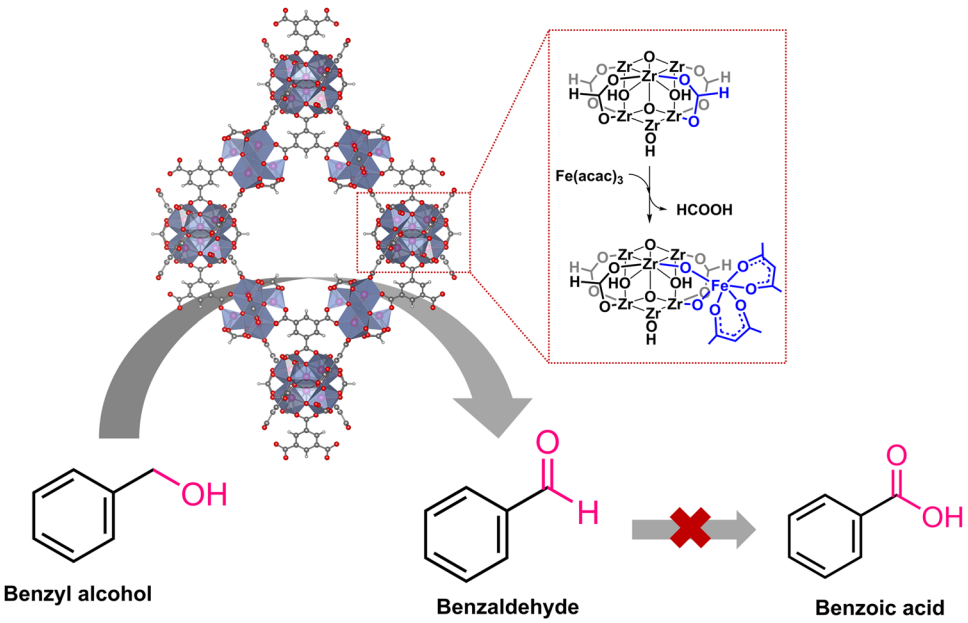

FIG. 1. Synthesis of Fe-grafted MOF-808 by incorporation of iron acetylacetonate complex into –OH Zr_6 node using metal acetylacetonate complexes.

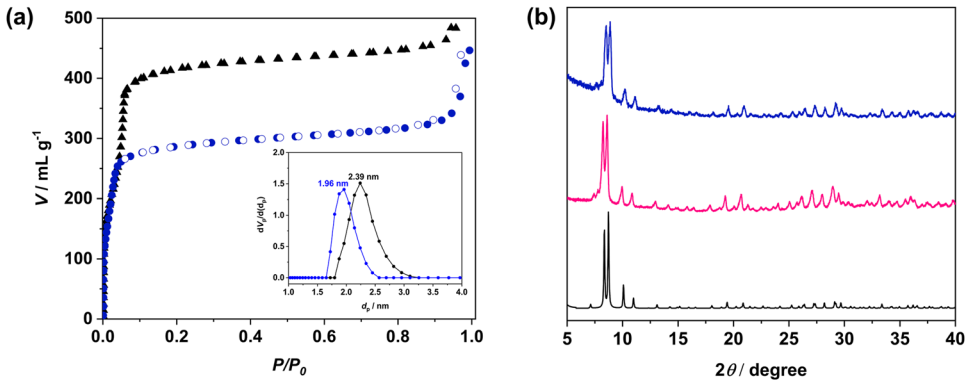

FIG. 2. (a) N_2 adsorption isotherms of MOF-808 (filled triangles) and Fe-MOF-808 (filled circles) at 77 K, and (b) from bottom to top, PXRD patterns of simulated MOF-808, MOF-808, and Fe-MOF-808.

To further elucidate the coordination environment of the covalently grafted Fe species, the acquired Fe-MOF-808 was subjected to analysis using X-ray absorption spectroscopy (XAS). As shown in Fig. 4(a), the X-ray absorption near-edge structure (XANES) spectrum of Fe-MOF-808 did not match with iron oxides but resembles to that of $Fe(acac)_3$, suggesting the grafting of Fe species as a metal complex rather than the metal oxides forms. However, the different XANES spectral features of Fe-MOF-808 to those of $Fe(acac)_3$ indicates that the octahedral coordination environment of Fe^{3+} in Fe-MOF-808 is distorted compared to a symmetric octahedral structure of $Fe(acac)_3$. The slightly shifted spectrum to the higher energy results from the different chemical species of the coordination environment. The Fourier transform of the extended X-ray absorption fine structures (EXAFS) [Fig. 4(b)] reveals that Fe^{3+} is monomerically bound to MOF-808. The EXAFS refinement was performed using the model where Fe^{3+} is located on the Zr node. The Fe–O, Fe–C, and Fe–Zr correlations taken from the model provide a good fit to the data with an *R*-factor of 0.1%. The presence of Fe–O–Zr correlation instead of Fe–O–Fe confirms the validity of the model. The incorporation of Fe species into the Zr node of MOF-808 is assisted by the addition of NEt_3, which facilitates the ligand exchange of acetylacetonate and the –OH group of the Zr node. The proposed mechanism on the grafting of $Fe(acac)_3$ to the Zr node and the roles of NEt_3 are shown in Fig. S1. The role of NEt_3 was proved by the unsuccessful grafting of $Fe(acac)_3$ in the absence of NEt_3.

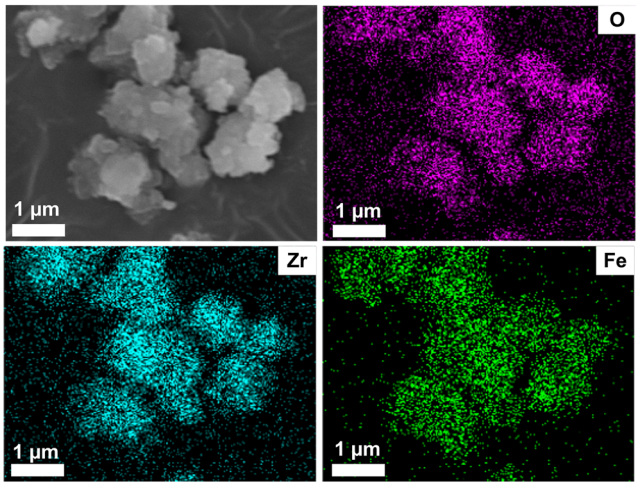

FIG. 3. SEM images and EDX mapping of Fe-MOF-808.

For the use of Fe-MOF-808 as a catalyst for the selective oxidation of benzyl alcohol, we first browsed through the feasibility of oxidation in the presence of tert-butyl hydroperoxide (TBHP) by Fe-MOF-808, $Fe(acac)_3$, and MOF-808. The HPLC chromatogram qualitatively shows that Fe-MOF-808 exhibits an enhancement on the catalytic activity among the others in terms of conversion and selectivity to benzaldehyde (Table I, entries 1–3 and 5). TBHP in the absence of MOFs shows adventitious oxidation of benzyl alcohol to both benzaldehyde and benzoic acid (57% vs 43% selectivity). Despite a lack of the incorporated metal ions, MOF-808 with TBHP can oxidize benzyl alcohol to benzaldehyde more selectively (98% selectivity) compared to the reaction with TBHP alone, reflecting that MOF-808 confers selectivity toward this oxidation to some degree. The oxidation reaction by MOF-808 is probably attributed to high Lewis acidity elicited by the defective Zr node, which can catalyze Meerwein-Pondorff-Varley reactions without additional metals doping.[36,37]

Fe-MOF-808 was further used as the catalyst for benzyl alcohol oxidation to benzaldehyde. To optimize the oxidation condition of Fe-MOF-808, the catalyst loading of Fe-MOF-808 was varied as follows: 3 mol. %, 6 mol. %, and 10 mol. %, and the 10 mol. % catalyst provided a catalytic performance as high as 12 mol. %. Therefore, the 10 mol. % catalyst is the optimal level for the catalytic reaction. For the amount of TBHP used, 2 M equivalents of TBHP was the lowest amount that allowed the complete conversion of benzyl alcohol. To explore the effect of solvents, CH_3CN/cyclohexane (1:1) was chosen based on the previous discussion that cyclohexane could expel water out of the reaction and prevent overoxidation of aldehyde to acid.[38,39] The conversion of benzyl alcohol is adversely aggravated by this mixed solvent system. By contrast, using only CH_3CN leads to high conversion and selectivity. To explore the optimal time and temperature, 90 °C is presumably the lowest temperature to let the reaction complete within 9 h, the time point at which shorter than the previously reported MOF catalyst using Pd/Au encapsulated nanoparticle UiO-66.[22] The selectivity of the benzaldehyde formation is maintained even at the higher temperature of 120 °C. Therefore, the optimized parameters for the reaction were 10 mol. %

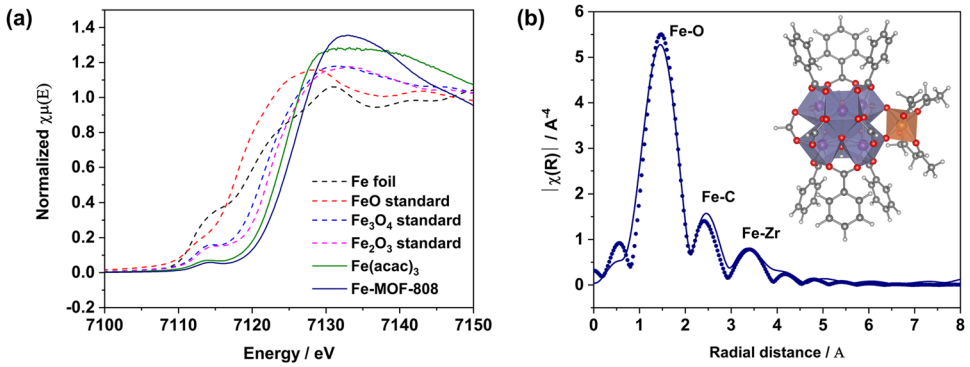

FIG. 4. (a) Fe *K*-edge XANES spectra of Fe-MOF-808 and reference compounds. (b) Fe *K*-edge EXAFS spectrum of Fe-MOF-808 (dots) and EXAFS spectrum simulated from the proposed DFT models (solid line).

TABLE I. Selective oxidation of benzyl alcohol to benzaldehyde. 10 mol. % catalyst, 2 eq. TBHP, and in CH_3CN.

Entry	Catalyst	Time (h)	Temp. (°C)	Conversion (%)	Benzaldehyde selectivity (%)
1	. . .	9	90	21	57
2	MOF-808	9	90	10	98
3	$Fe(acac)_3$	9	90	10	83
4	Fe-UiO-66	9	90	32	100
5	Fe-MOF-808	9	90	99	96

Fe-MOF-808 with 2 M eq. TBHP at 90 °C for 9 h in CH_3CN. The optimal condition was applied to homogeneous catalyst $Fe(acac)_3$ (Table I, entry 5). The reaction mechanism of the oxidation of benzyl alcohol to benzaldehyde is generally proposed based on the binding of benzyl alcohol to the unsaturated metal sites, and the reaction proceeds through the heterolytic cleavage of chemical bonds. In cases of Fe-MOF-808, benzyl alcohol could not bind to the fully coordinated Fe^{3+} sites. There is no acetylacetonate removed during the catalytic reactions as confirmed by the EXAFS spectrum of the used catalyst. The reaction on Fe-MOF-808 tends to occur by the homolytic cleavage assisted by TBHP and Fe^{3+} to generate the radical intermediates (Fig. S2). Fe^{3+} acts as the single-electron transfer catalyst to generate the benzylic carbon radicals in the reaction. The radical-based mechanism also explains the high selectivity to benzaldehyde with a trace amount of benzoic acid being formed. Benzaldehyde radicals, which are the key intermediates to the overoxidation to benzoic acid, are not stable in the catalytic systems. In addition, when compared to Fe-grafted UiO-66 (Table I, entries 4 and 5), Fe-MOF-808 also outcompetes Fe-UiO-66, owing to the larger pore aperture of MOF-808 that allows the substrate to enter the pore more readily.

To test the leaching of Fe-MOF-808 after use in catalysis, the leaching of Fe^{3+} into the reaction liquid phase was tested by filtering the catalyst out of the reaction after 3 h, and the reaction was continued without the catalyst. The filtered reaction mixture proceeds in the direction in which benzoic acid is generated at a relatively higher amount, while the levels of benzyl alcohol and benzaldehyde tend to decrease slightly. This reflects that TBHP left in the reaction nonspecifically oxidizes benzaldehyde. This nonselective oxidation strongly suggested that the Fe catalytic site of the reaction was not leached into the solution. To further confirm the catalyst leaching, the filtrates at 3 h and 6 h from each reaction time were also subjected to ICP analysis and the Fe level was not detected under the limit of detection. The reusability of the catalyst was also assayed by removing the Fe-MOF-808 catalyst by centrifugation. The used Fe-MOF-808 was then collected and reused in the three subsequent runs. The results revealed that Fe-MOF-808 catalyst can be recycled at least four times without structural disruption according to its retained PXRD patterns and without decreasing in the catalytic activity (Fig. S3).

CONCLUSIONS

In this work, the Fe-MOF-808 catalyst was simply prepared by a one-pot reaction using iron acetylacetonate. The Fe^{3+} species was incorporated at the Zr node of MOF-808 by a ligand exchange of acetylacetonate and the –OH group at the Zr node as structurally elucidated by XAS techniques (XANES and EXAFS). Fe-MOF-808 provides excellent conversion of benzyl alcohol and selectivity to benzaldehyde. In addition, Fe-MOF-808 surpassed the prototype Zr-based MOF, Fe-UiO-66 along with its own precursor, $Fe(acac)_3$. The stability of Fe-MOF-808 was confirmed by the leaching test, and the catalyst can be recycled for at least four times without deactivation. To this end, our simple and facile method of Fe^{3+} incorporation into the Zr nodes of MOF-808 paves an important step in the molecular engineering of the catalyst.

SUPPLEMENTARY MATERIAL

See the supplementary material for proposed mechanisms on the graft of $Fe(acac)_3$ to MOF-808, proposed mechanisms for the catalytic reactions, XRD patterns of Fe-MOF-808 before and after a catalytic reaction, and EXAFS fitting parameters for Fe-MOF-808.

ACKNOWLEDGMENTS

This research was supported by Research Grant for New Scholar from the Thailand Research Fund and Office of the Higher Education Commission (Grant No. MRG6080278 to K.K.) and a postdoctoral fellowship from Vidyasirimedhi Institute of Science and Technology (to W.J.). We acknowledge the Synchrotron Light Research Institute (Public Organization), SLRI, for provision of beamtime, and we would like to thank the staff of beamline 1.1W for their assistance. We appreciate the support of the Institute for Integrated Cell-Material Sciences-Vidyasirimedhi Institute of Science and Technology Research Center.

REFERENCES

[1] R. A. Sheldon, I. W. C. E. Arends, and A. Dijksman, Catal. Today **57**, 157–166 (2000).
[2] F. Brühne and E. Wright, "Benzaldehyde," in *Ullmann's Encyclopedia of Industrial Chemistry* (Wiley VCH, Weinheim, 2011), pp. 223–235.
[3] A. Nozaki, T. Yasuoka, Y. Kuwahara, T. Ohmichi, K. Mori, T. Nagase, H. Y. Yasuda, and H. Yamashita, Ind. Eng. Chem. Res. **57**, 5599–5605 (2018).
[4] Y. Yan, Y. Chen, X. Jia, and Y. Yang, Appl. Catal., B **156-157**, 385–397 (2014).
[5] A. Savara, I. Rossetti, C. E. Chan-Thaw, L. Prati, and A. Villa, ChemCatChem **8**, 2482–2491 (2016).
[6] M. Khawaji and D. Chadwick, ChemCatChem **9**, 4353–4363 (2017).
[7] I. Bauer and H.-J. Knölker, Chem. Rev. **115**, 3170–3387 (2015).
[8] N. A. Vermeulen, M. S. Chen, and M. Christina White, Tetrahedron **65**, 3078–3084 (2009).
[9] M. S. Chen and M. C. White, Science **318**, 783 (2007).
[10] G. Zhao, F. Yang, Z. Chen, Q. Liu, Y. Ji, Y. Zhang, Z. Niu, J. Mao, X. Bao, P. Hu, and Y. Li, Nat. Commun. **8**, 14039 (2017).
[11] O. Singh, P. Gupta, A. Singh, A. Maji, U. P. Singh, and K. Ghosh, Appl. Organomet. Chem. **33**, e4825 (2019).
[12] S. Higashimoto, R. Shirai, Y. Osano, M. Azuma, H. Ohue, Y. Sakata, and H. Kobayashi, J. Catal. **311**, 137–143 (2014).
[13] K. Lagerblom, P. Wrigstedt, J. Keskiväli, A. Parviainen, and T. Repo, ChemPlusChem **81**, 1160–1165 (2016).
[14] Q. Yan, Y. C. Fang, Y. X. Jia, and X. H. Duan, New J. Chem. **41**, 2372–2377 (2017).
[15] T. Gadzikwa, G. Lu, C. L. Stern, S. R. Wilson, J. T. Hupp, and S. T. Nguyen, Chem. Commun. **2008**(43), 5493–5495.
[16] J. Chen, K. Li, L. Chen, R. Liu, X. Huang, and D. Ye, Green Chem. **16**, 2490–2499 (2014).
[17] H. Fei, J. Shin, Y. S. Meng, M. Adelhardt, J. Sutter, K. Meyer, and S. M. Cohen, J. Am. Chem. Soc. **136**, 4965–4973 (2014).
[18] A. Bétard and R. A. Fischer, Chem. Rev. **112**, 1055–1083 (2012).
[19] R. B. Getman, Y.-S. Bae, C. E. Wilmer, and R. Q. Snurr, Chem. Rev. **112**, 703–723 (2012).
[20] P. Horcajada, R. Gref, T. Baati, P. K. Allan, G. Maurin, P. Couvreur, G. Férey, R. E. Morris, and C. Serre, Chem. Rev. **112**, 1232–1268 (2012).
[21] A. Das and D. M. D'Alessandro, CrystEngComm **17**, 706–718 (2015).
[22] X. Li, Z. Guo, C. Xiao, T. W. Goh, D. Tesfagaber, and W. Huang, ACS Catal. **4**, 3490–3497 (2014).
[23] Z. Li, N. M. Schweitzer, A. B. League, V. Bernales, A. W. Peters, A. B. Getsoian, T. C. Wang, J. T. Miller, A. Vjunov, J. L. Fulton, J. A. Lercher, C. J. Cramer, L. Gagliardi, J. T. Hupp, and O. K. Farha, J. Am. Chem. Soc. **138**, 1977–1982 (2016).
[24] A. W. Peters, Z. Li, O. K. Farha, and J. T. Hupp, ACS Nano **9**, 8484–8490 (2015).
[25] D. Yang, S. O. Odoh, T. C. Wang, O. K. Farha, J. T. Hupp, C. J. Cramer, L. Gagliardi, and B. C. Gates, J. Am. Chem. Soc. **137**, 7391–7396 (2015).
[26] H. G. T. Nguyen, N. M. Schweitzer, C.-Y. Chang, T. L. Drake, M. C. So, P. C. Stair, O. K. Farha, J. T. Hupp, and S. T. Nguyen, ACS Catal. **4**, 2496–2500 (2014).
[27] S. T. Madrahimov, J. R. Gallagher, G. Zhang, Z. Meinhart, S. J. Garibay, M. Delferro, J. T. Miller, O. K. Farha, J. T. Hupp, and S. T. Nguyen, ACS Catal. **5**, 6713–6718 (2015).
[28] J. K. F. Buijink, J. J. M. van Vlaanderen, M. Crocker, and F. G. M. Niele, Catal. Today **93-95**, 199–204 (2004).
[29] S. Lwin and I. E. Wachs, ACS Catal. **4**, 2505–2520 (2014).
[30] I. E. Wachs and C. A. Roberts, Chem. Soc. Rev. **39**, 5002–5017 (2010).
[31] H. Furukawa, F. Gándara, Y.-B. Zhang, J. Jiang, W. L. Queen, M. R. Hudson, and O. M. Yaghi, J. Am. Chem. Soc. **136**, 4369–4381 (2014).
[32] B. Ravel and M. Newville, J. Synchrotron Radiat. **12**, 537–541 (2005).
[33] K. Momma and F. Izumi, J. Appl. Crystallogr. **44**, 1272–1276 (2011).
[34] Y. Shao, Z. Gan, E. Epifanovsky, A. T. B. Gilbert, M. Wormit, J. Kussmann, A. W. Lange, A. Behn, J. Deng, X. Feng, D. Ghosh, M. Goldey, P. R. Horn, L. D. Jacobson, I. Kaliman, R. Z. Khaliullin, T. Kuś, A. Landau, J. Liu, E. I. Proynov, Y. M. Rhee, R. M. Richard, M. A. Rohrdanz, R. P. Steele, E. J. Sundstrom, H. L. Woodcock, P. M. Zimmerman, D. Zuev, B. Albrecht, E. Alguire, B. Austin, G. J. O. Beran, Y. A. Bernard, E. Berquist, K. Brandhorst, K. B. Bravaya, S. T. Brown, D. Casanova, C.-M. Chang, Y. Chen, S. H. Chien, K. D. Closser, D. L. Crittenden, M. Diedenhofen, R. A. DiStasio, H. Do, A. D. Dutoi, R. G. Edgar, S. Fatehi, L. Fusti-Molnar, A. Ghysels, A. Golubeva-Zadorozhnaya, J. Gomes, M. W. D. Hanson-Heine, P. H. P. Harbach, A. W. Hauser, E. G. Hohenstein, Z. C. Holden, T.-C. Jagau, H. Ji, B. Kaduk, K. Khistyaev, J. Kim, J. Kim, R. A. King, P. Klunzinger, D. Kosenkov, T. Kowalczyk, C. M. Krauter, K. U. Lao, A. D. Laurent, K. V. Lawler, S. V. Levchenko, C. Y. Lin, F. Liu, E. Livshits, R. C. Lochan, A. Luenser, P. Manohar, S. F. Manzer, S.-P. Mao, N. Mardirossian, A. V. Marenich, S. A. Maurer, N. J. Mayhall, E. Neuscamman, C. M. Oana, R. Olivares-Amaya, D. P. O'Neill, J. A. Parkhill, T. M. Perrine, R. Peverati, A. Prociuk, D. R. Rehn, E. Rosta, N. J. Russ, S. M. Sharada, S. Sharma, D. W. Small, A. Sodt, T. Stein, D. Stück, Y.-C. Su, A. J. W. Thom, T. Tsuchimochi, V. Vanovschi, L. Vogt, O. Vydrov, T. Wang, M. A. Watson, J. Wenzel, A. White, C. F. Williams, J. Yang, S. Yeganeh, S. R. Yost, Z.-Q. You, I. Y. Zhang, X. Zhang, Y. Zhao, B. R. Brooks, G. K. L. Chan, D. M. Chipman, C. J. Cramer, W. A. Goddard, M. S. Gordon, W. J. Hehre, A. Klamt, H. F. Schaefer, M. W. Schmidt, C. D. Sherrill, D. G. Truhlar, A. Warshel, X. Xu, A. Aspuru-Guzik, R. Baer, A. T. Bell, N. A. Besley, J.-D. Chai, A. Dreuw, B. D. Dunietz, T. R. Furlani, S. R. Gwaltney, C.-P. Hsu, Y. Jung, J. Kong, D. S. Lambrecht, W. Liang, C. Ochsenfeld, V. A. Rassolov, L. V. Slipchenko, J. E. Subotnik, T. Van Voorhis, J. M. Herbert, A. I. Krylov, P. M. W. Gill, and M. Head-Gordon, Mol. Phys. **113**, 184–215 (2015).
[35] J. Jiang, F. Gándara, Y.-B. Zhang, K. Na, O. M. Yaghi, and W. G. Klemperer, J. Am. Chem. Soc. **136**, 12844–12847 (2014).
[36] A. H. Valekar, K.-H. Cho, S. K. Chitale, D.-Y. Hong, G.-Y. Cha, U. H. Lee, D. W. Hwang, C. Serre, J.-S. Chang, and Y. K. Hwang, Green Chem. **18**, 4542–4552 (2016).
[37] E. Plessers, G. Fu, C. Y. X. Tan, D. E. De Vos, and M. B. J. Roeffaers, Catalysts **6**, 104 (2016).
[38] A.-K. C. Schmidt and C. B. W. Stark, Org. Lett. **13**, 4164–4167 (2011).
[39] R. Noyori, M. Aoki, and K. Sato, Chem. Commun. **2003**(16), 1977–1986.